A 3D CHANNEL FLOW SIMULATION AT $RE_\tau = 180$ USING A RATIONAL LES MODEL

P. FISCHER AND T. ILIESCU
Mathematics and Computer Science Division
Argonne National Laboratory
9700 S. Cass Ave., Argonne, IL 60439

Abstract. This paper presents numerical results obtained by applying an LES model based on a rational (subdiagonal Padé) approximation in the wave number space. We used a spectral element code to test this LES model, a coarse DNS, and the Smagorinsky model with Van Driest damping in the numerical simulation of a 3D channel flow at $Re_\tau = 180$. The corresponding results were compared with the fine DNS simulation of Moser, Kim, and Mansour.

1. Introduction

Introduced in 1970 by Deardorff [4], Large Eddy Simulation (LES) is one of the most promising approaches to the numerical simulation of turbulent flows. LES has a rich history, being successfully developed and applied to a wide range of applications by the engineering and geophysics communities.

LES is based on the idea that the large scales in the flow are essential, being responsible for the important engineering quantities (heat transfer, mixing, etc.), whereas the small scales are important because of their effect on the large scales. Another important assumption in LES is that the small scales of turbulence are more isotropic and more universal than the large scales.

The usual LES starts by convoluting the Navier-Stokes equations (NSE) with a spatial filter g_δ:

$$\overline{\mathbf{u}}_t + \nabla \cdot (\overline{\mathbf{u}}\overline{\mathbf{u}}) - Re^{-1}\Delta\overline{\mathbf{u}} + \nabla\overline{p} = \overline{\mathbf{f}}, \tag{1}$$

where $\overline{\mathbf{u}} = g_\delta * \mathbf{u}$ is the variable of interest. The filtered NSE (1) do not form a closed system, and most LES research has been directed at modeling the subgrid-scale (SGS) stress

$$\tau = \overline{\mathbf{u}}\overline{\mathbf{u}} - \overline{\mathbf{u}}\ \overline{\mathbf{u}}. \tag{2}$$

Arguably the most popular class of SGS models is the eddy viscosity type, based on (variants of) Smagorinsky's model [24],

$$\tau = -(C_s\delta)^2\ |\nabla^s\overline{\mathbf{u}}|\ \nabla^s\overline{\mathbf{u}}, \tag{3}$$

where δ is the radius of the filter and $\nabla^s \overline{\mathbf{u}} = \frac{1}{2}(\nabla \overline{\mathbf{u}} + \nabla \overline{\mathbf{u}}^T)$. Smagorinsky proposed (3) with C_s a constant, but the most successful models have been those in which C_s is computed dynamically (the dynamic subgridscale eddy viscosity model [9] and its variants).

Other successful LES models include the scale-similarity models, the mixed models (scale-similarity models coupled with an eddy-viscosity model to properly dissipate energy), and the RNG models.

Despite its undeniable achievements, LES still poses numerous challenges, many of them at a very fundamental level. One of these challenges is the need for more mathematical consistency, which would provide the means for sounder mathematical and numerical analysis for the corresponding LES models. Other fundamental challenges are the LES boundary conditions, the influence of the filter on the SGS model, commutation errors in filtering, numerical errors, and numerical validation. A growing current of opinion in the LES community favors the need for new approaches that could answer these fundamental challenges.

The LES model used in this paper is based on an approximation rather than a physical analogy. This model has evolved in several steps. First, in 1974 Leonard [16] developed a continuum model of $\overline{\overline{\mathbf{u}}\,\overline{\mathbf{u}}}$

$$\overline{\overline{\mathbf{u}}\,\overline{\mathbf{u}}} = \overline{\mathbf{u}}\,\overline{\mathbf{u}} + \frac{\delta^2}{4\gamma}\Delta(\overline{\mathbf{u}}\,\overline{\mathbf{u}}) + O(\delta^4), \tag{4}$$

where δ is the radius of the filter and γ is a parameter in the Gaussian filter. Next, in 1979 Clark, Ferziger, and Reynolds [3] developed an analogous model for the "cross terms" $\overline{\overline{\mathbf{u}}\mathbf{u}'} + \overline{\mathbf{u}'\overline{\mathbf{u}}}$, where $\mathbf{u}' := \mathbf{u} - \overline{\mathbf{u}}$ represents the turbulent fluctuations. The approach used in the derivation of these models involved taking the Fourier transform of the corresponding terms, approximating the Fourier transform of the Gaussian filter $\hat{g_\delta}$, dropping the terms of order $O(\delta^4)$ and, finally, taking the inverse Fourier transform of the resulting approximations. Noticing that the approximation by Taylor series of $\hat{g_\delta}$ actually *increases* the high wave number components, Galdi and Layton [8] developed a new LES model based on a rational ((0,1) Padé) approximation of $\hat{g_\delta}$, which preserves the decay of the high wave number components. The resulting LES model, which will be called in the sequel the "Rational" LES model, reads as follows:

$$\begin{cases} \mathbf{w}_t - Re^{-1}\Delta\mathbf{w} + \nabla\cdot(\mathbf{w}\mathbf{w}) + \nabla q + \nabla\cdot\left[\left(-\frac{\delta^2}{4\gamma}\Delta + I\right)^{-1}\left(\frac{\delta^2}{2\gamma}\nabla\mathbf{w}\nabla\mathbf{w}\right)\right] = \overline{\mathbf{f}} & \text{in } \Omega, \\ \mathbf{w}(\mathbf{x},0) = \overline{\mathbf{u}}_0(\mathbf{x}) & \text{in } \Omega, \\ \text{Boundary Conditions} & \text{on } \partial\Omega, \end{cases}$$

where $(\mathbf{w}, q)$ are proposed as an approximation to $(\overline{\mathbf{u}}, \overline{p})$, $\Omega \subseteq \mathbb{R}^d$ $(d = 2, 3)$, and

$$(\nabla\mathbf{w}\nabla\mathbf{w})_{i,j} = \sum_{l=1}^{d} \frac{\partial \mathbf{w}_i}{\partial \mathbf{x}_l}\frac{\partial \mathbf{w}_j}{\partial \mathbf{x}_l}. \tag{5}$$

A sound mathematical analysis [2] and the first steps for a numerical validation [12] were provided for the "Rational" LES model (5) coupled with a Smagorinsky model with a very small coefficient C_s (for alternatives to the Smagorinsky model, see [14]).

This paper presents numerical results for the "Rational" LES model (5) applied to the 3D channel flow test problem at a Reynolds number based on the wall shear velocity $Re_\tau = 180$.

2. Numerical Setting

The 3D channel flow (Figure 1) is one of the most popular test problems for the investigation of the wall bounded turbulent flows. We will compare our numerical results with the extensive data existing for this test problem (both Direct Numerical Simulation (DNS) and LES). The computational domain is periodic in the streamwise (x) and spanwise (z) directions, and the pressure gradient that drives the flow is adjusted dynamically to maintain a constant mass flux through the channel. We selected the periodic domain sizes (x and z) as $L_x = 2\pi$, $L_z = \frac{4}{3}\pi$, and we chose unity as the channel half-width ($\delta_{channel} = 1$). We employed in our calculations a $40 \times 49 \times 40$ quadrature grid. The length scale δ is computed as $\delta = \sqrt[3]{\Delta_x\ \Delta_z\ \Delta_y(y)}$, where Δ_x and Δ_z are twice the largest spaces between the Gauss-Lobatto-Legendre (GLL) points in the x and z directions, respectively, and $\Delta_y(y)$ is inhomogeneous and is computed as an interpolation function that is zero at the wall and is twice the normal meshsize for the elements near the wall and for those in the center of the channel. For the "Rational" LES model (5) we chose $\gamma = 6$ (the usual choice for the Gaussian filter).

We compared the "Rational" LES model (5) with the Smagorinsky model with Van Driest damping (see [18]). The Smagorinsky model with Van Driest damping is obtained by modifying the usual Smagorinsky model (3) to reduce the eddy viscosity in the near-wall region

$$\tau = -[C_s\delta(1 - exp(-y^+/A^+))]^2\ |\nabla^s\overline{\mathbf{u}}|, \tag{6}$$

where $y^+ = (\delta_{channel} - |y|)u_\tau/\nu$ is the nondimensional distance from the wall, C_s is the Smagorinsky constant, and A^+ is a constant. Here u_τ is the wall-shear velocity, $u_\tau = \sqrt{\tau_{wall}/\rho}$, in which ρ is the density, and τ_{wall} is the wall-shear. In our calculations we made the usual choices: $C_s = 0.1$ and $A^+ = 25$.

The numerical simulations were performed using a spectral element code based on the $\mathbb{P}_N - \mathbb{P}_{N-2}$ velocity and pressure spaces introduced by Maday and Patera [17]. The domain is decomposed into $8 \times 10 \times 8$ elements, as shown in Figure 2. The velocity is continuous across element interfaces and is represented by Nth-order tensor-product Lagrange polynomials based on the GLL points. The pressure is discontinuous and is represented by tensor-product polynomials of degree $N - 2$. Time stepping is based on an operator-splitting of the discrete system, which leads to separate convective, viscous, and pressure subproblems without the need for ad-hoc pressure boundary conditions. A filter, which removes 5% of the highest velocity mode, is used to stabilize the Galerkin formulation [7]. Details of the discretization and solution algorithm are given in [5], [6].

We applied initial conditions consisting of the parabolic mean flow (Poiseuille flow), on which a 2D Tollmien-Schlichting (TS) mode of 2% amplitude and a 3D TS mode of 1% amplitude were superimposed.

In our numerical experiments we considered, as a first step, homogeneous boundary conditions for the "Rational" LES model (5). The mathematical and numerical investigation of more realistic (slip-with-friction) boundary conditions in the LES context began in [22], [13].

The numerical results include plots of the following time- and plane-averaged quantities: the mean streamwise velocity $\ll \overline{u} \gg$, the x,y-component of the Reynolds stress $\ll u'v' \gg$, and the

rms values of the streamwise $\ll u'u' \gg$, wall-normal $\ll v'v' \gg$, and spanwise $\ll w'w' \gg$ velocity fluctuations, where $< \cdot >$ denotes plane (xz) averaging, $\ll \cdot \gg$ denotes time and plane (xz) averaging, the fluctuating quantities f' are calculated as $f' = f - \ll f \gg$, and a "+" superscript denotes the variable in wallunits.

3. Results and Conclusions

These numerical results were the basis for *a posteriori* tests: we compared them with the fine DNS simulation of Moser, Kim and Mansour [19].

Figure 3 shows the mean streamwise velocity; note the almost perfect overlapping of the results corresponding to the two methods ("Rational" LES and Smagorinsky model with Van Driest damping). The same behavior can be observed in the x, y-component of the Reynolds stress in Figure 4, with a slight improvement for the "Rational" LES model.

Figures 5–7, containing the rms values for the three velocity components, merit a more detailed discussion.

The rms values of the streamwise velocity fluctuations in Figure 5 show a better (closer to the fine DNS benchmark results in [19]) behavior for the "Rational" LES model. Near the wall this improvement is clearer, the two models performing similarly away from the wall.

Figure 6 shows the rms values of the wall-normal velocity fluctuations. Here, the Smagorinsky model with Van Driest damping performs slightly better near the wall, and consistently better between the near-the-wall region and the center of the channel. Toward the center of the channel, the LES model performs slightly better.

The rms values of the spanwise velocity fluctuations in Figure 7 are consistently better for the LES model, with the exception of a very short portion close to the center of the channel.

In conclusion, the LES model performs better near the wall (with the exception of the rms values of the wall-normal velocity fluctuations), whereas the Smagorinsky model with Van Driest damping performs better closer to the center of the channel (with the exception of the rms values of the spanwise velocity fluctuations). The two models are comparable in accuracy.

Further research should be directed at the investigation of additional terms accounting for the discarded $O(\delta^4)$ terms in the "Rational" LES model, as well as to the influence of the length scale δ in the spectral element implementation of the "Rational" LES model.

4. Acknowledgments

This work was supported in part by the Mathematical, Information, and Computational Sciences Division subprogram of the Office of Advanced Scientific Computing Research, U.S. Dept. of Energy, under Contract W-31-109-Eng-38.

We thank Prof. R. Moser for helpful communications that improved this paper.

References

1. Aldama, A.A. (1990) *Filtering Techniques for Turbulent Flow Simulation*. Lecture Notes in Engineering **56**, Springer-Verlag, ed. by C. A. Brebbia and S. A. Orszag.
2. Berselli, L.C., Galdi, G.P., Layton, W.J. and Iliescu, T. (2001) Mathematical Analysis for a Large Eddy Simulation Model, preprint

3. Clark, R. A., Ferziger, J.H. and Reynolds, W.C. (1979) Evaluation of Subgrid Scale Models Using an Accurately Simulated Turbulent Flow, *J. Fluid Mech.* **91**, pp. 1–16
4. Deardorff, J.W. (1970) A Numerical Study of Three-Dimensional Turbulent Channel Flow of Large Reynolds Numbers, *J. Fluid Mech.* **41**, pp. 453–480
5. Fischer, P.F. (1997) An Overlapping Schwarz Method for Spectral Element Solution of the Incompressible Navier-Stokes Equations, *J. of Comp. Phys.* **133**, pp. 84–101
6. Fischer, P.F., Miller, N.I. and Tufo, H.M. (2000) An Overlapping Schwarz Method for Spectral Element Simulation of Three-Dimensional Incompressible Flows, in *Parallel Solution of Partial Differential Equations*. Springer-Verlag, ed. by P. Björstad and M. Luskin, pp. 159-181.
7. Fischer, P.F. and Mullen, J.S. (2001) Filter-Based Stabilization of Spectral Element Methods *Comptes rendus de l'Académie des sciences Paris, t. 332, -Série I - Analyse numérique*, pp. 265–270
8. Galdi, G.P. and Layton, W.J. (2000) Approximating the Larger Eddies in Fluid Motion II: A Model for Space Filtered Flow, *Math. Methods and Models in Applied Sciences* **10**, pp. 343–350
9. Germano, M., Piomelli, U., Moin, P. and Cabot, W. (1991) A Dynamic Subgridscale Eddy Viscosity Model, *Phys. Fluids A* **3**, pp. 1760–1765
10. Geurts, B.J. (1997) Inverse Modeling for Large-Eddy Simulation, *Phys. Fluids* **9**, pp. 3585–3587
11. Hughes, T.J.R., Oberai, A.A. and Mazzei, L. (2001) Large Eddy Simulation of Turbulent Channel Flows by the Variational Multiscale Method, *Phys. Fluids* **13**, pp. 1784–1799
12. Iliescu, T., John, J., Layton, W.J., Matthies, G. and Tobiska L. (2001) A Numerical Study of a Class of LES Models, preprint.
13. Iliescu, T., John, J. and Layton, W.J. (2001) Convergence of Finite Element Approximation of Large Eddy Motion, preprint.
14. Iliescu, T. and Layton, W.J. (1998) Approximating the Larger Eddies in Fluid Motion III: The Boussinesq Model for Turbulent Fluctuations, *An. St. Univ."Al. I. Cuza"* **44**, pp. 245–261
15. Kim, J., Moin, P. and Moser, R. (1987) Turbulence Statistics in Fully Developed Channel Flow at Low Reynolds Number, *J. Fluid Mech.* **177**, pp. 133–166
16. Leonard, A. (1974) Large Eddy Simulation of Turbulent Fluid Flows, *Adv. in Geophysics* **18A**, pp. 237–248
17. Maday, Y. and Patera, A.T. (1989) Spectral Element Methods for the Navier-Stokes Equations, in *State of the Art Surveys in Computational Mechanics*, ASME, New York, ed. by A. K. Noor, pp. 71–143
18. Moin, P. and Kim, J. (1982) Numerical Investigation of Turbulent Channel Flow, *J. Fluid Mech.* **118**, pp. 341–377
19. Moser, D.R., Kim, J. and Mansour, N.N. (1999) Direct Numerical Simulation of Turbulent Channel Flow up to $Re_\tau = 590$, *Phys. Fluids* **11**, pp. 943–945
20. Piomelli, U. (1993) High Reynolds Number Calculations Using the Dynamic Subgrid-Scale Stress Model, *Phys. Fluids A* **5**, pp. 1484–1490
21. Sagaut, P. (2001) *Large Eddy Simulation for Incompressible Flows*. Springer Verlag, Berlin.
22. Sahin, N. (2001) New Perspectives on Boundary Conditions for Large Eddy Simulation, preprint.
23. Sarghini, F., Piomelli, U. and Balaras, E. (1999) Scale-Similar Models for Large-Eddy Simulations, *Phys. Fluids* **11**, pp. 1596–1607
24. Smagorinsky, J. (1963) General Circulation Experiments with the Primitive Equation: I The Basic Experiment, *Mon. Wea. Rev.* **91**, pp. 216–241
25. Stolz, S., Adams, N.A. and Kleiser, L. (2001) An Approximate Deconvolution Model for Large-Eddy Simulation with Application to Incompressible Wall-Bounded Flows, *Phys. Fluids* **13**, pp. 997–1015

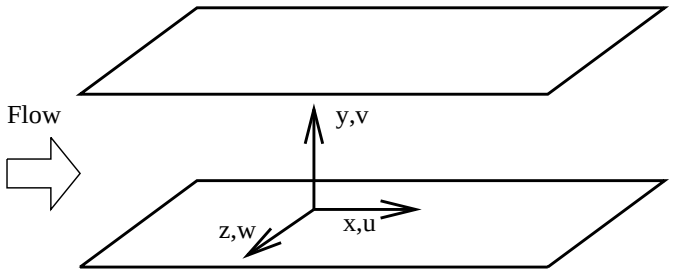

Figure 1. Problem setup for the channel flow.

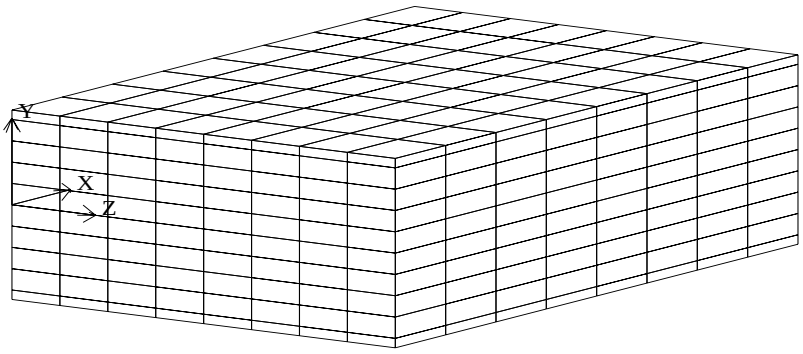

Figure 2. Spectral element mesh.

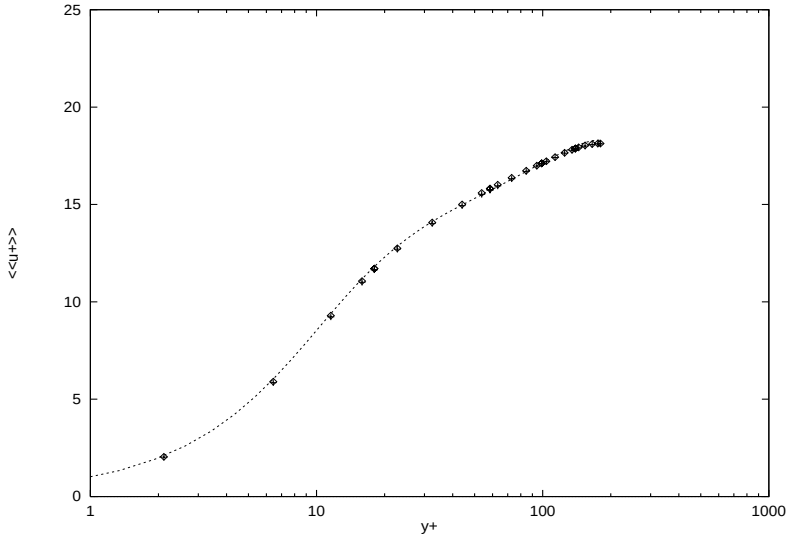

Figure 3. Mean streamwise velocity; ... fine DNS, $\diamond$ Smagorinsky with Van Driest damping, + "Rational" LES.

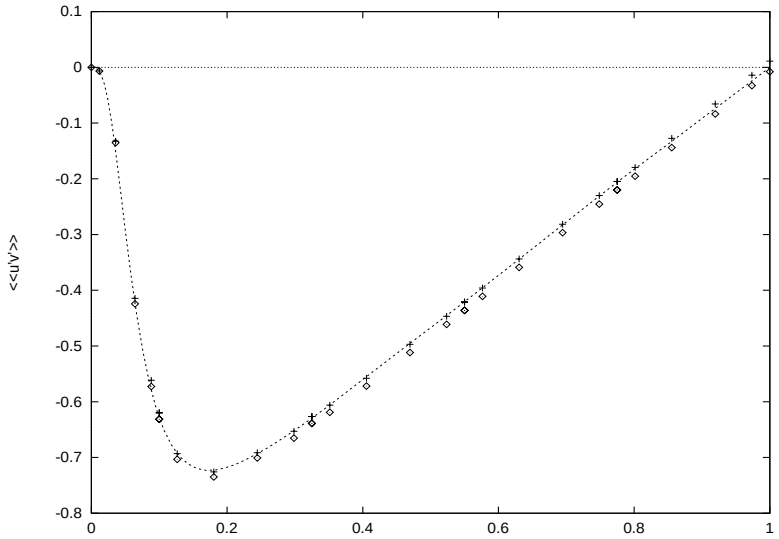

Figure 4. x, y-component of the Reynolds stress; ... fine DNS, $\diamond$ Smagorinsky with Van Driest damping, + "Rational" LES.

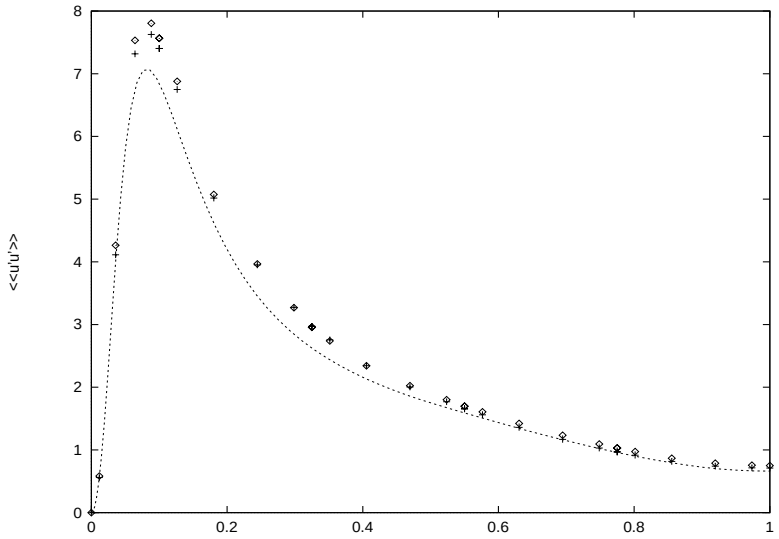

Figure 5. rms values of streamwise velocity fluctuations; ... fine DNS, $\diamond$ Smagorinsky with Van Driest damping, + "Rational" LES.

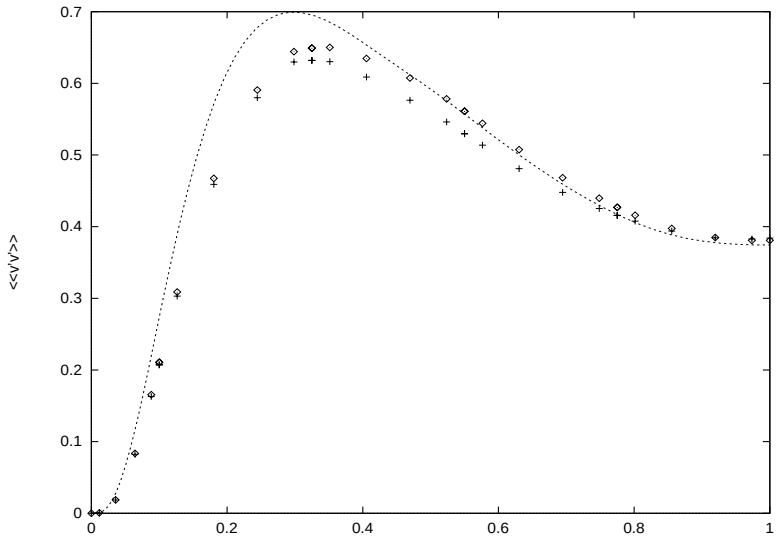

Figure 6. rms values of wall-normal velocity fluctuations; ... fine DNS, ◇ Smagorinsky with Van Driest damping, + "Rational" LES.

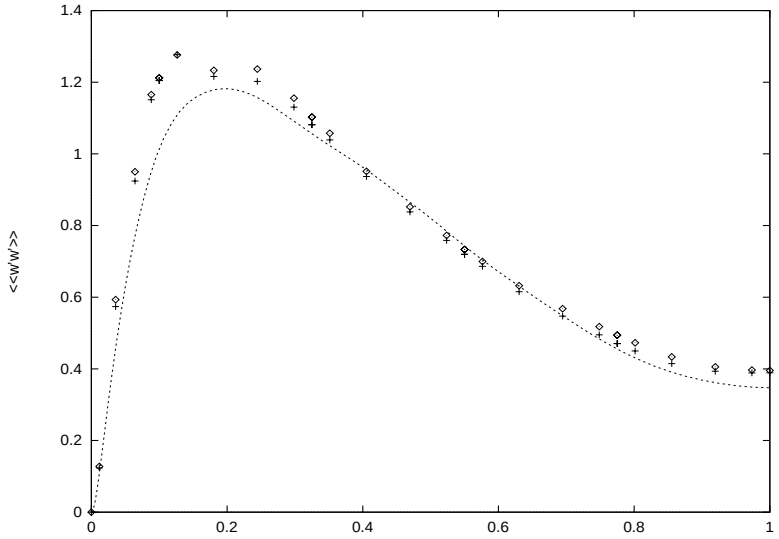

Figure 7. rms values of spanwise velocity fluctuations; ... fine DNS, ◇ Smagorinsky with Van Driest damping, + "Rational" LES.